Development of a Black-Box Compressor Model that Captures Vapor-Injection Compared Against Established Black-Box Models

Amjid Khan[1]*, Craig R. Bradshaw[2]

[1,2]Center for Integrated Building Systems, Oklahoma State University,
Stillwater, Oklahoma, US
[1]amjid.khan@okstate.edu, [2]craig.bradshaw@okstate.edu

* Corresponding Author

ABSTRACT

In high temperature gradients regions, vapor compression systems operate at very high-pressure ratios, results in higher discharge temperatures and a reduction in system performance. Economized vapor injection compressors are used to avoid these issues, yet a precise predictive map for various compressor technologies with minimal data and relatively better performance is unclear. This paper establishes a black-box compressor model to accurately predict compressor evaporator mass flow rate, injection mass ratio, and power in compressors with a single vapor injection port. This model is compared against three legacy models from literature and the ANN model, for reference. All five models are evaluated based on their ability to predict the aforementioned metrics. The proposed black-box model can predict the relevant metrics all within 5% Mean Absolute Percentage Error (MAPE). Additionally, a refrigerant sensitivity analysis is performed with the black-box model. The model is trained with data from R410A and used to predict the performance of the same compressor with R454B, and vice versa. The model can predict evaporator mass flow within 3%, power within 2%, and injection mass ratio within 3% MAPE.

1. INTRODUCTION

When the temperature difference between indoor and outdoor temperatures is significant the COP of heat pumps is greatly reduced, attributed mostly to compressor behavior. The large temperature differences create equivalently large pressure ratios and compressors have resultingly low volumetric and compressor isentropic efficiencies in these scenarios. Therefore, compressor power consumption increases significantly, and the discharge temperature reaches inappropriately high values affecting the compressor reliability and endurance. This is one major reason heat pumps are limited in severe climate conditions (Khan and Bradshaw, 2022). Heat pumps that include economization have the potential to address these limitations but modeling the vapor injected compressors needed for these heat pumps is currently challenging for equipment manufacturers.

To address the limitations in compressors, various cycle modifications such as intercooling, cascade refrigeration, and flash tank economization have been proposed, with vapor injection presenting a promising solution. Economized vapor injection cycles have been considered to achieve a reduction in specific compressor work and increase in capacity, resulting in increased system COP (Xu et al., 2011). This technique consists of injecting refrigerant from the condenser outlet to an intermediate pressure, optimized to maximize cycle efficiency (Mathison et al., 2011).

Economized cycles have become the basis of many new heat pump designs, particularly those targeting cold-climate operation (Residential CCHP Challenge DOE, 2021), and have demonstrated benefits through experimental study. Wang et al., (2009b) studied the performance of 11kW R410A heat pump system with a two-stage vapor injected scroll compressor, experimentally, and set a general principle for the design and operation of heat pump systems. Results showed that maximum COP of the system can be achieved when the injection pressure is equal to the injection pressure at which the cooling capacity is maximum. It is also concluded from the study that heating capacity gain varies from 13% to 33%, as the ambient temperature decreases from 16.7°C to -17.6°C, showing the significance of vapor injected compressors at high temperature lift. Similar results were captured during experimental investigation of vapor injected compressor showing significance of economization and vapor injection by (Yang et al., 2015, Cho et al., 2002). Overall, the benefits of economization and vapor injection included, well-demonstrated benefits to COP and cold-climate operation.

The compressor serves as the pivotal component within the vapor compression system, embodying its complexity. Scroll compressors are the predominant compressor technology of choice in unitary equipment, including heat pumps.

Scroll compressors provide several advantages including independent compression chambers inside scroll compressors, making it easy to incorporate vapor injection in it by providing many options for injection port location that maximizes cycle efficiency. Most research on vapor injection is focused on its application in Scroll compressors (Feng et al., 2009; Lumpkin et al., 2018a; Moesch et al., 2016.; Tello Oquendo et al., 2016a; Tello-Oquendo et al., 2019; B. Wang et al., 2009; X. Wang et al., 2009a). A common theme of compression-based studies is a wide variety of modeling approaches for compressors with vapor injection with no clear and obvious best way to model scroll compressors for system development.

The black-box model is one of the modelling approaches, which does not rely on specific physical information regarding compression and injection processes within the compressor. Instead, these models typically comprise polynomial equations, where the coefficients are adjusted to match experimental data. The primary challenge associated with black-box models is the issue of overfitting. These models cannot predict the performance for unseen data and perform poorly in case of extrapolation (Hu et al., 2020). Black box models for vapor injected compressors in literature have only been developed for scroll compressors and its performance evaluation for multiple compressor technologies is missing, discussed in detail in section 3 (Navarro et al., 2013, Tello-Oquendo et al., 2017a, Lumpkin et al., 2018b). In addition to all these black-box models, machine learning approaches such as ANN, have been used for systems and compressor performance prediction in HVAC systems (Gabel and Bradshaw, 2023, Ziviani et al., 2018, Ledesma et al., 2015; Ma et al., 2020; Sanaye et al., 2011; Yousaf et al., 2022).

In summary, all existing black-box models have been exclusively characterized for vapor injection scroll compressor technology, with no consideration given to other compressor technologies for performance evaluation. Furthermore, these models require substantial amounts of data, often exceeding 10 data points, to predict the performance of variable-speed compressors accurately. Additionally, there is a lack of literature regarding refrigerant-flexible models, which can be trained using data for one refrigerant (such as R410A) and subsequently applied to predict the performance of a drop-in refrigerant (such as R454B) using the same model coefficients.

The objective of this study is to bridge this gap in the literature by proposing a model that demonstrates refrigerant flexibility, a reduced number of coefficients, and applicability to both scroll and rotary compressors with generalized accuracy of less than 5%, compared with experimental data. The proposed model will be compared against models developed by Oquendo, Lumpkin, Navarro, and an ANN model (Tello-Oquendo et al. 2017; Lumpkin et al. 2018; Navarro et al. 2013; Ledesma et al. 2015). Each model is trained using in-house data on vapor injection rotary and scroll compressors collected on both R410A and R454B. The experimental data collection, detailed descriptions of the reference models and the develop model are presented in the following sections.

2. EXPERIMENTAL COLLECTION AND COMPILATION OF DATA SETS

Experimental data is compiled from 6 vapor injected compressors of 2 technology types (rotary and scroll), using 3 refrigerants for a total of 195 data points to be used for model training and evaluation. The majority of this data is collected by the authors (116 data points), with supplemental data collected from the literature.

2.1 Experimental data collection – in house data

For the in-house data collection, the hot-gas bypass load stand has been used for collection of data on two scroll and rotary compressors with refrigerants, R410A and R454B. The load stand is capable of testing both traditional and economized compressors at saturated suction temperature as low as -34.44 °C (-30 °F) and saturated discharge temperature as high as 60 °C (140 °F). The design capacity for the load stand is 1-5 tons compressor capacity. Complete operational details and uncertainty of the load stand is presented in (Khan and Bradshaw 2024).

2.2 Compressor Selection and Test Matrix Generation

Performance data for two compressor technologies, scroll and rotary, are collected with two working fluids, R410A and R454B with a total number of 116 data points. The compressors are commercially available hermetic compressors originally designed for operation with R410A. The scroll compressor has a rated capacity of 5 tons and the rotary 3.25 tons. The complete test matrix was developed based on one factor at a time design of experiments method. The final test matrix collected data at evaporating temperatures ranging from -1.11 °C to 10 °C (-30 °F to 50 °F), condensing ranging from 23.8 °C to 54.44 °C (75 °F to 130 °F), superheat from 2.8 °C to 16.7 °C (5 °F to 30 °F), and speeds from 1800 rpm to 6000 rpm.

Supplemental experimental data was also collected from literature including data for a scroll compressor from Dardenne et al., (2015b) and Tello-Oquendo et al., (2017b), both tested with R407C as shown in Table 1, a summary

of the data sets for the analysis of the models with compressor type, refrigerant, number of data points, and collection standard is shown. The full data set is then divided into two subsets for each model performance evaluation, training and testing data set.

Table 1: Compiled experimental data sets.

Compressor Type	Capacity	Refrigerant	Data Points	Collection Standard
Rotary (In-House)	3.25 tons	R410A	29	ASHRAE 23.1
Rotary (In-House)	3.25 tons	R454B	29	ASHRAE 23.1
Scroll (In-House)	05 tons	R410A	29	ASHRAE 23.1
Scroll (In-House)	05 tons	R454B	29	ASHRAE 23.1
Scroll (Dardenne et al., 2015b)	03 tons	R407C	63	ASHRAE 23.1
Scroll (Oquendo et al., 2017b)	4.74 tons	R407C	16	ISO

3. SELECTED MODELS DESCRIPTION

This section provides an overview of the 5 selected models chosen for vapor injection compressor performance evaluation. The models included in the analysis are Artificial Neural Network (ANN) as a baseline model, and four other models are Navarro et al., (2013b), Tello-Oquendo et al., (2017b), Lumpkin et al., (2018b), and model developed for this work, referred to as the 'proposed model'. While numerous output variables are of interest in a compressor model, the focus of this discussion is on the prediction of compressor injection mass ratio, evaporator mass flow rate, and compressor power.

3.1.1 Artificial Neural Network

The ANN serves as the benchmark for comparing with other black-box models. The ability of an ANN to obtain connections between data is exceptional. However, it is difficult to standardize an ANN and make it re-producible for many compressors, so it is not a useful candidate for final model selection. Therefore, the use of the ANN is to represent a very good model prediction and used solely for comparative purposes.

The ANN consists of interconnected layers and nodes that process numerical inputs. This machine learning model relies on an optimization algorithm that adjusts the weights and biases within the network by utilizing backpropagation of error through the loss function. In this study, the Limited Memory Breydon-Flecher-Goldfarb-Shanno (lbfgs) optimizer is employed which is usually more stable, while the rectified linear activation function is used, which accurately and efficiently transforms negative inputs to zero and preserves positive values. The mean absolute percent error (MAPE) is selected as the loss function. Four inputs, namely suction pressure, injection pressure, discharge pressure, and compressor speed, are fed into the network, while the network outputs the mass flow rate and compressor power. Each model comprises an input layer, a hidden layer, and an output layer. The dataset for model training consists of randomly selected data, with 80% allocated for training and 20% for testing. During training, the data is passed through the input layer, and the optimization algorithm is applied, after configuring the hyperparameters. The final results are then obtained. Table 2 summarizes the artificial neural network architecture considered for this study.

Table 2: ANN Model Architecture

Parameters	Values
Machine Learning Package	Scikit-learn, Spyder, Python
Inputs	4
Outputs	2
Hidden Layers	1
Nodes Per Layer	45
Activation Function	Rectified Linear
Optimizer	Limited Memory BFGS

3.1.2 Navarro Model

The model from Navarro et al., (2013b) is a black-box model which only captures the injection mass flow rate. The correlation for injection mass flow rate is a first-order polynomial function of evaporating mass flow rate ($\dot{m}_e$) and injection to evaporator pressure ratio (P_{inj}/P_e). The model inputs are evaporating mass flow rate, injection pressure (P_{inj}), and evaporating pressure (P_e). The number of data points required are 13 to tune the coefficients for this model.

There is no specific vapor injection compressor needed to run the model. However, the training data needed to train the model, there must be at least 3 data points to curve fit the injection mass flow rate ($\dot{m}_{inj}$). The model functional form is shown in Table 3 for injection and evaporator mass flow rate.

Table 3: Formulation for Navarro Model

Parameter	Equation
Injection mass flow rate	$\dot{m}_{inj} = K_0 + K_1\dot{m}_e + K_2\left(\frac{P_{inj}}{P_e}\right)\dot{m}_e$
Evaporator mass flow rate	$\dot{m}_e = a_1 + a_2T_e + a_3T_c + a_4T_e^2 + a_5T_eT_c + a_6T_c^2 + a_7T_e^3 + a_8T_e^2T_c + a_9T_eT_c^2 + a_{10}T_c^3$

3.1.3 Tello-Oquendo Model

The model from Tello-Oquendo et al., (2017b) is a black-box model, which captures compressor power, total mass flow rate, and injection mass flow rate. It follows the exact same formulation of AHRI 10 coefficient map with one extra coefficient. The Tello-Oquendo model adds injection temperature (T_{inj}) as an additional term for compressor power prediction. This model is also third-order polynomial, and it is a function of evaporating temperature, condensing temperature and injection temperature summarized in table 4. In this formulation compressor power prediction needs 11 data points, which results in 11 tuned coefficients from ($a_1 - a_{11}$). In this model, the computational efforts are minimal and just like all other black-box models, it does not require any information about the compressor geometry. The injection to evaporation mass flow rate ratio is a first order polynomial equation and a function of injection to evaporating pressure ratio. Compressor geometrical description is not required for this model as well.

Table 4: Formulation for Tello-Oquendo Model

Parameters	Values
Compressor power	$\dot{E} = a_1 + a_2T_e + a_3T_c + a_4T_e^2 + a_5T_eT_c + a_6T_c^2 + a_7T_e^3 + a_8T_e^2T_c + a_9T_eT_c^2 + a_{10}T_c^3 + a_{11}T_{inj}$
Evaporator flowrate	$\dot{m}_e = a_1 + a_2T_e + a_3T_c + a_4T_e^2 + a_5T_eT_c + a_6T_c^2 + a_7T_e^3 + a_8T_e^2T_c + a_9T_eT_c^2 + a_{10}T_c^3$
Injection mass ratio	$\frac{\dot{m}_{inj}}{\dot{m}_e} = A + B\left(\frac{P_{inj}}{P_e}\right)$

3.1.4 Lumpkin Model

The Lumpkin model from (Lumpkin et al., 2018b) is a black-box model, which uses dimensionless groups, codified from Buckingham-PI, for mapping compressor power consumption, injection mass flow ratio. The mapping of compressor power output ratio and injection mass flow ratio was created as output group, and appropriate dimensionless input groups were considered for each normalized output PI group listed in Table 5. The suction temperature is normalized with ambient temperature and refrigerant critical temperature. The enthalpy difference ($\Delta h_{suc,sh}$) at the compressor inlet is characterized by the enthalpy difference between measured inlet enthalpy and saturated liquid enthalpy at the same pressure. The enthalpy difference ($\Delta h_{inj,sh}$) at the compressor injection point is characterized by the enthalpy difference between measured injection enthalpy and saturated liquid enthalpy at the same pressure. The theoretical maximum compressor power ($\dot{W}_{max}$) was calculated using equation in Table 5, assuming a power factor of 0.85, supply voltage of 206 V and the maximum current is 18 A.

To tune the coefficients from $C_0 - C_9$, total 10 data points are required. Compared to all the models mentioned till now, this model is more complex and the same as other black-box models, it does not require any information about the compressor type and compressor size.

Table 5: Formulation of Lumpkin Model

Parameters	Values
Injection mass flow ratio	$\frac{\dot{m}_{inj}}{\dot{m}_e} = C_0\left(\frac{f_{power}}{f_{nominal}}\right)^{C_1}\left(\frac{\Delta h_{inj,sh}}{\Delta h_{inj,fg}}\right)^{C_2}\left(\frac{P_{inj}}{P_{suc}}\right)^{C_3}\left(\frac{T_{suc}}{T_{amb}}\right)^{C_4}\left(\frac{P_{dis}}{P_{suc}}\right)^{C_5}$ $(\frac{\Delta h_{suc,sh}}{\Delta h_{suc,fg}})^{C_6}(\frac{P_{dis}}{P_{crit}})^{C_7}(\frac{P_{suc}}{P_{crit}})^{C_8}(\frac{T_{suc}}{T_{crit}})^{C_9}$
Compressor power ratio	$\frac{\dot{W}_{act}}{\dot{W}_{max}} = C_0\left(\frac{f_{power}}{f_{nominal}}\right)^{C_1}\left(\frac{\dot{m}_{inj}}{\dot{m}_e}\right)^{C_2}\left(\frac{P_{inj}}{P_{suc}}\right)^{C_3}\left(\frac{T_{suc}}{T_{amb}}\right)^{C_4}\left(\frac{P_{dis}}{P_{suc}}\right)^{C_5}$ $(\frac{\Delta h_{suc,sh}}{\Delta h_{suc,fg}})^{C_6}(\frac{P_{dis}}{P_{crit}})^{C_7}(\frac{P_{suc}}{P_{crit}})^{C_8}(\frac{T_{suc}}{T_{crit}})^{C_9}$
Maximum Compressor Power	$\dot{W}_{max} = \cos(\theta)\sqrt{3} I_{ph,max}\Delta V$

3.1.5 Proposed Model

The present study proposes a model for the evaluation of the vapor injection compressor performance to predict the compressor power, total mass flow rate, and injection mass flow ratio. This model is also a black-box model in nature, and second-order polynomial with 11 coefficients. In this model the total mass flow rate going through the condenser ($\dot{m}_c$) and compressor power consumption is a function of condenser pressure, evaporator pressure, and injection pressure. The total number of coefficients for total mass flow rate and compressor power comprised of 11 coefficients each and it require 11 data points each to tune these coefficients from ($a_0 - a_{10}$). For fixed speed vapor injected compressor analysis, will require 9 data points to tune the coefficients excluding the speed terms. For injection mass ratio, the proposed model also uses Tello-Oquendo et al., (2017b) with a modification for variable speed compressor performance prediction as shown in Table 6.

Like all other black-box models considered, it requires 11 data points for variable speed vapor injected compressor power and evaporator mass flow rate prediction. Additionally, the representation of the proposed model as a function of pressures is much more universal compared with temperature-based formulations. Unlike temperatures, compressor sees refrigerant at evaporating pressure at suction, compresses it to discharge seeing condensing pressure. The compressor power consumption as a function of pressures is much more independent of the refrigerant and much better representative of the compressor (Marchante-Avellaneda et al., 2023).

Table 6: Formulation for the Proposed Model

Parameters	Values
Compressor Power	$\dot{W}_{map} = a_0 + a_1P_e + a_2P_c + a_3P_e^2 + a_4P_c^2 + a_5\omega + a_6\omega^2 + a_7P_eP_c + a_8P_eP_c^2 + a_9P_cP_e^2 + a_{10}P_{inj}$
Injection Mass Ratio	$\frac{\dot{m}_{inj}}{\dot{m}_e} = a + b * \left(\frac{P_{inj}}{P_e}\right) + c * \left(\frac{\omega_{act}}{\omega_{nom}}\right)$
Evaporator Flow Rate	$\dot{m}_e = a_0 + a_1P_e + a_2P_c + a_3P_e^2 + a_4P_c^2 + a_5\omega + a_6\omega^2 + a_7P_eP_c + a_8P_eP_c^2 + a_9P_cP_e^2 + a_{10}P_{inj}$
Mass Balance	$\dot{m}_c = \dot{m}_e + \dot{m}_{inj}$

3.2 Error Metric to Evaluate Model Performance

Each model is trained then evaluated for its ability to predict compressor power, evaporator, and injection mass flow rates using the method shown graphically in Figure 1. Each model is initially trained using a training dataset comprising 11 data points. Following the training phase, the performance of the trained model is evaluated by comparing its predictions against the corresponding test data obtained from experiments as described in Sections 2.2. The evaluation of model performance is quantified using the Mean Absolute Percentage Error (MAPE), which serves as a metric to measure the accuracy and effectiveness of the models in predicting the desired outcomes,

$$MAPE = \frac{100}{n}\sum_{i=1}^{n}\left|\frac{Y_{true,i}-Y_{predict,i}}{Y_{true,i}}\right|, \quad (1)$$

where n is the total number of data points in the data set, i is each data point, $Y_{true,i}$ and $Y_{predict,i}$ are the model measured data value and model predicted data value for any performance parameter. The MAPE is calculated for both the evaporator mass flow rate and injection mass ratio as well as compressor power.

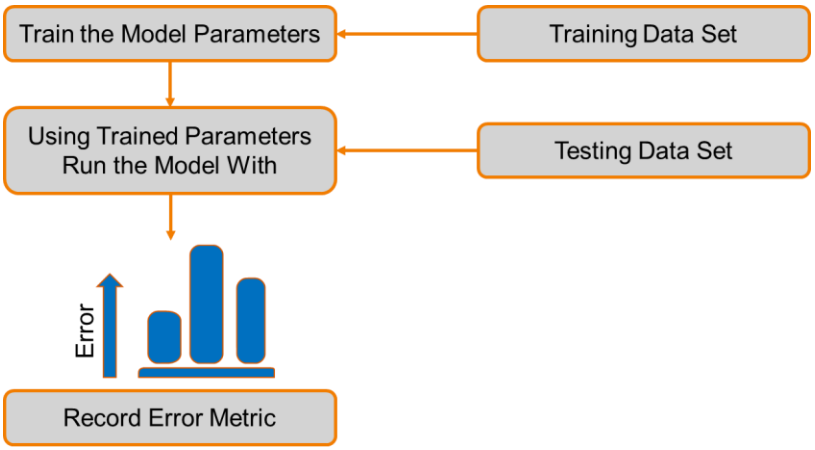

Figure 1: Model training and evaluation methodology used in this study.

4. RESULTS

The results presented in this section show each model's ability to predict injection mass ratio, evaporator mass flow rate, and compressor power. The over-arching objective is a model that can predict these parameters within 5% of experiments with as little data as possible and the goodness of each model is evaluated based on this criterion.

4.1 Compressor Power Consumption

In Figure 2, a comparative analysis of predictive models used for compressor power prediction is presented as a heat map representing MAPE. While all the models predicted performance well, however the Proposed Model consistently demonstrated superior predictive capability. The MAPE values associated with the Proposed Model are all lower than 1% compared to the other models, except for the scroll R410A data, highlighting its effectiveness in capturing compressor power. The ANN model performs the next best showing low MAPE values except for the scroll R454B data set, which shows the MAPE of 2.4%. The Oquendo model prediction is reasonably good as well, and Lumpkin model performing the worst with the MAPE more than 1% in most of the cases. This comparative assessment underscores the enhanced predictive capabilities of the Proposed Black Box Model, presenting it as a more promising model. Its ability to yield more accurate predictions under 2% MAPE of compressor power holds significant implications for optimizing compressor performance.

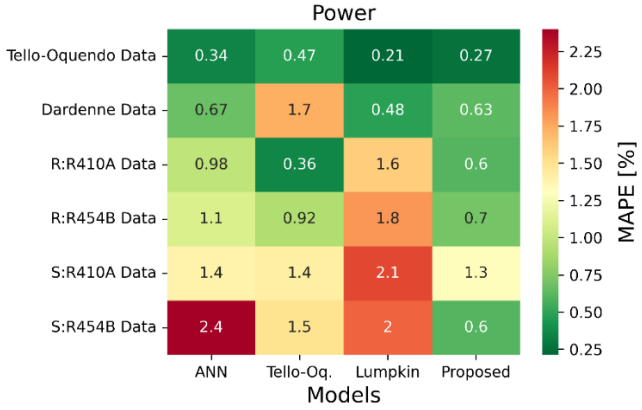

Figure 2: Heatmap showing MAPE of model predictions of compressor power for each dataset.

4.2 Evaporator and Injection Mass Flow Rate

Figure 3 is a heat map for evaporator mass flow rate representing the MAPE for each of the models using all the data sets mentioned in Table 1. Results show that evaporator mass flow rate is captured well by the Proposed model except rotary compressor R454B data with the MAPE of 2.6%. As per the model selection criteria, the MAPE for all the models is less than 5% in evaporator mass flow rate prediction. The results for Tello-Oquendo, Navarro, and Lumpkin are similar, since all these models are similar for predicting the evaporator mass flow rate. However, the proposed model predicted the evaporator mass flow rate under 3% MAPE, which is better than all other models except the ANN.

In Figure 3, a comparative analysis of predictive models used for injection mass ratio prediction is presented as a heat map representing MAPE. The injection mass ratio MAPE values for the Proposed model are lower than 2% compared to all other models, even better than benchmark ANN model. The Lumpkin model failed to perform in predicting the injection mass ratio. The Lumpkin model exhibits errors above 5% MAPE in injection mass ratio prediction for both scroll and rotary compressor technologies. For injection mass ratio prediction, the lowest MAPE achieved was 0.93% for Tello-Oquendo data set utilizing R407C by the proposed model. Navarro and Oquendo models MAPE is lower compared to Lumpkin model. This comparison shows that the Proposed Model predicts evaporator and injection mass flow rates better than all other models, even better than benchmark ANN model.

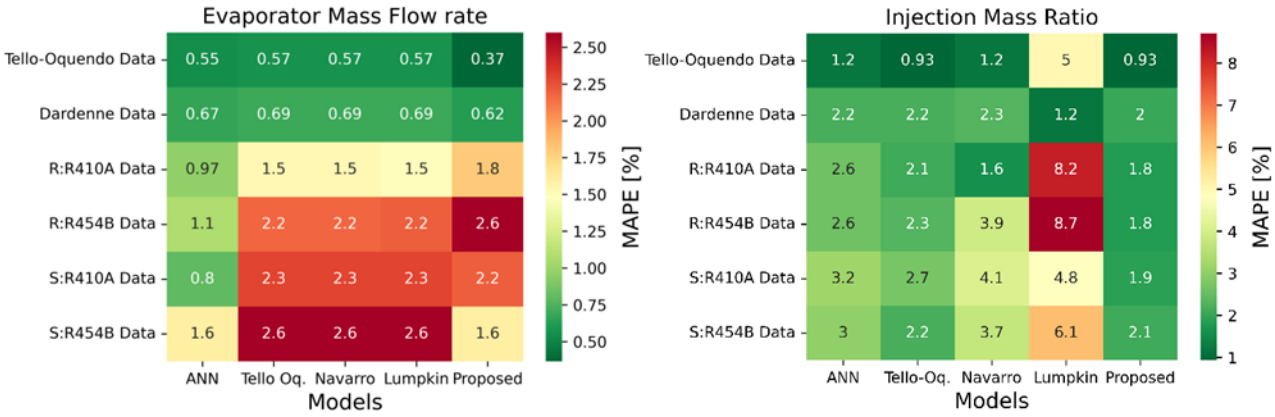

Figure 3: Heatmaps showing MAPE of model predictions of evaporator mass flow rate (left) and injection mass ratio (right) for each dataset.

4.3 Refrigerant Flexibility Analysis

Refrigerant flexibility was assessed for both injection mass ratio and compressor power consumption. The experimental data obtained for this study includes identical datasets for both R454B and R410A on two compressors, a scroll and a rotary. These results were used to train each model with either R410A or R454B data and then attempt to predict the injection mass ratio and compressor power consumption of the other refrigerant. The same training data sets as used in the other analysis are used. The results, depicted in Figures 4, showcase the compressor power consumption, and injection mass ratio predictions.

For compressor power consumption prediction shown in Figure 4 (left), the Proposed model exhibited the most accurate predictions with the lowest MAPE values for both refrigerants except the ANN, but it is worth noting that ANN model was used as a benchmark for the comparison of all models. For training with R410A and testing with R454B, the MAPE is 1.85%, and for training with R454B and testing with R410A, the MAPE is 1.4%. The worst performing model in evaluating the refrigerant flexibility analysis is the Lumpkin model with MAPE higher than 20%. Similarly, in the case of injection mass ratio prediction depicted in Figure 4 (right), the Proposed model demonstrated the lowest MAPE values among all models except the ANN, indicating predictive accuracy for both refrigerants. Specifically, for training with R410A and testing with R454B, the MAPE is 2.84%, while for training with R454B and testing with R410A, the MAPE is 1.87%.

Comparatively, the Lumpkin model showed significantly higher MAPE values, indicating a substantial deviation compared to all other models and a lower level of accuracy in predicting refrigerant flexibility for both injection mass ratio and compressor power consumption.

These findings underscore the effectiveness of the Proposed model in accurately predicting refrigerant flexibility, making it a valuable tool for predicting the performance of vapor-injected rotary compressors when transitioning between different refrigerants.

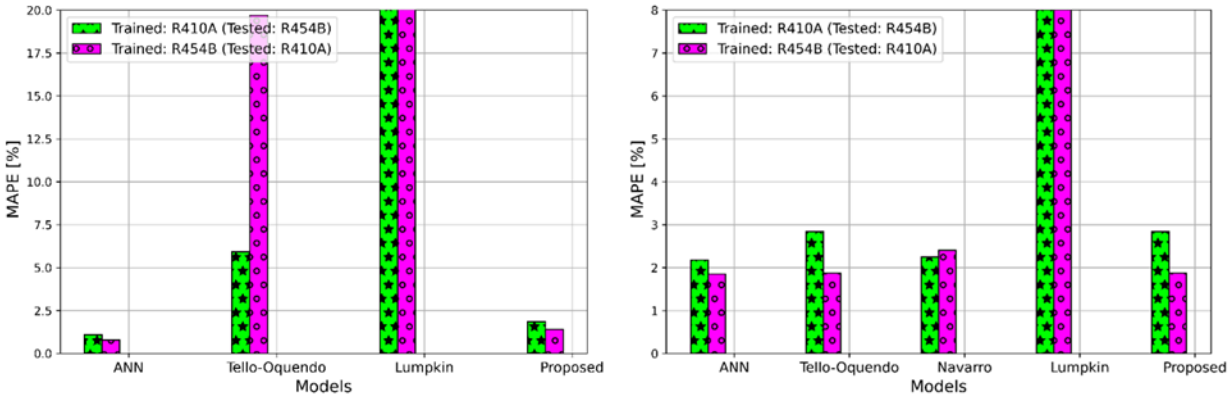

Figure 4: Compressor Power Consumption (left) and injection mass ratio (right)

5. DISCUSSION

The Tello-Oquendo model yielded more consistent performance in predicting compressor power and mass flow rates. The performance prediction of Tello-Oquendo is less than 3% for mass flow rates and compressor power except the refrigerant flexibility analysis, in which the MAPE is higher than 3%. The Lumpkin model failed to demonstrate good results in the case of injection mass ratio for rotary compressor R410A and R454B data exceeding 5% MAPE. In comparison to Lumpkin model, Navarro model manages to predict MAPE less than 5% for injection mass ratio. Overall, the Proposed model surpassed all other models by achieving a MAPE less than 2% for all three key output parameters: compressor power, evaporator mass flow rate, and injection mass ratio. Additionally, it outperformed other models in refrigerant flexibility analysis except ANN, which is used as a benchmark model.

The Lumpkin model is a complex combination of normalized inputs with a total number of 10 coefficients for both mass flow rate and power prediction. It requires 10 training data points for each model along with the calculation of thermophysical properties such as enthalpies. However, with all this added complexity, it failed to predict injection mass ratio with MAPE less than 5%. Besides that, it faded to capture the refrigerant flexibility analysis as well. The Tello-Oquendo model is 11 coefficient model for each compressor power and evaporator mass flow rate and is much better at predicting these output parameters. However, a notable limitation of the Tello-Oquendo model is its inability to capture variable speed data. The ANN model was the best performing since that was the baseline model and has much more accurate prediction for both mass flow rate and compressor power. The Proposed model outperformed all other models in predicting all output parameters. It has 11 coefficients and can capture variable speed data with 11 data points. In general, black-box models are not capable of refrigerant flexibility analysis since it doesn't have any physics or geometrical information, however, the performance of the Proposed model was similar to the ANN model in refrigerant flexibility analysis, exhibiting MAPE below 5% for both compressor power and injection mass ratio.

6. CONCLUSION

This study presents an analysis of the predictive capabilities of 4 black box models for vapor-injected compressors from literature and a newly proposed model. Each model is evaluated in its ability to predict compressor power, evaporator mass flow rate, and injection mass ratio. Additionally, this study also evaluates the models ability to predict the performance of a similar refrigerant when trained with data on a different refrigerant.

Notably, the proposed model emerges as a novel contribution, utilizing compressor suction pressure, discharge pressure, and injection pressure as input variables to establish an exceptionally effective predictive framework for compressor performance prediction. Quantitative evaluation, employing MAPE, shows the consistent performance of the proposed model across various datasets, notably surpassing the legacy models, like the Navarro (Navarro et al., 2013b), Tello-Oquendo (Tello-Oquendo et al., 2017b), and the Lumpkin Models (Lumpkin et al., 2018b).

In the case of compressor power prediction, the proposed model with same number of coefficients predicted the performance much better than all other models for both fixed and variable speed data. In comparison to the proposed model, the Tello-Oquendo model cannot capture variable speed since it does not have variable speed term in it and secondly, proposed model outperformed it for fixed speed data as well. The Lumpkin model is a complex combination of normalized inputs requiring 10 data points to tune the coefficients, however it failed to predict the performance better than all other models. Furthermore, in terms of evaporator mass flow rate prediction, the proposed model consistently proves its significance, achieving the lowest MAPE values across all the datasets, affirming its accuracy.

Additionally, the assessment of refrigerant flexibility for injection mass ratio and compressor power consumption is critical. The Proposed model performs better than other models, showcasing minimum MAPE for both refrigerants. For instance, in compressor power prediction, the Proposed model obtained a MAPE of 1.85% (training with R410A and testing with R454B) and 1.4% (training with R454B and testing with R410A). In contrast, the Lumpkin Model displayed considerably higher MAPE values, indicating its diminished accuracy.

7. MODEL LIMITATIONS AND FUTURE OUTLOOK

The models investigated in this work have limitations stemming from performance prediction. The model with better prediction capabilities should require minimal data. To this end, Proposed model require the same amount of data as any other black box model i.e. 11 data points but with relatively better performance and can also capture variable speed data. Analogous to typical black box models, it does not include geometrical features or fundamental physics equations in the analysis, rendering it bad in extrapolation and is sensitive to the type of training data. The proposed model does not have any fundamental physics equations, which is why the MAPE for refrigerant flexibility analysis is also high but relatively better than any other black box model studied here.
Future work based on the results presented herein will be developing a vapor injection compressor model, that is inspired from physical compression phenomena such as polytropic process, having the capability to capture interpolation, extrapolation and refrigerant flexibility analysis for multiple compressor technologies i.e., rotary, scroll and spool compressors. Furthermore, this future model will necessitate minimal data points for training while adhering to the same methodological approach employed in this study to facilitate comprehensive comparisons.

NOMENCLATURE

$\dot{m}_{inj}$	Mass flow rate through the injection line	[kg/s]
$\dot{m}_{dis}$	Mass flow rate at the compressor discharge	[kg/s]
$\dot{m}_{suc}$	Mass flow rate at the compressor suction	[kg/s]
$m_e^{\cdot}$	Mass flow rate through evaporator	[kg/s]
p_{cond}	Condensing pressure	[kPa]
p_{inj}	Injection Pressure	[kPa]
p_{evap}	Evaporating Pressure	[kPa]
p_{crit}	Critical Pressure	[kPa]
T_e	Evaporating Temperature	[°C]
T_c	Condensing temperature	[°C]
T_{inj}	Injection temperature	[°C]
$f_{nominal}$	Nominal frequency	[Hz]
Δh	Enthalpy difference	[kJ/kg]
$\dot{W}_{max}$	Maximum theoretical work	[kW]
$\dot{W}_{act}$	Actual work	[kW]
I	Current	[A]
ΔV	Potential difference	[volt]

Abbreviations

ASHRAE	American Society of Heating, Refrigeration, and Air Conditioning Engineers
AHRI	Air-Conditioning, Heating, and Refrigeration Institute
MAPE	Mean Absolute Percentage Error
COP	Coefficient of performance

Greek Symbols

ω	Compressor speed	[rpm]

REFERENCES

Cho, H., Chung, J. T., & Kim, Y. (2003). *Influence of liquid refrigerant injection on the performance of an inverter-driven scroll compressor*. *International Journal of Refrigeration*, *26*(1), 87-94.

Dardenne, L., Fraccari, E., Maggioni, A., Molinaroli, L., Proserpio, L., & Winandy, E. (2015a). Semi-empirical modelling of a variable speed scroll compressor with vapour injection. *IJR*, *54*(1905), 76–87.

Feng, C., Kai, W., Shouguo, W., Ziwen, X., & Pengcheng, S. (2009). Investigation of the heat pump water heater using economizer vapor injection system and mixture of R22/R600a. *IJR*, *32*(3), 509–514.

Gabel, K. S., & Bradshaw, C. R. (2023). Evaluation and quantification of compressor model predictive capabilities under modulation and extrapolation scenarios. *International Journal of Refrigeration*, *149*, 1–10.

Hu, M., Xiao, F., & Cheung, H. (2020). Identification of simplified energy performance models of variable-speed air conditioners using likelihood ratio test method. *Science and Technology for the Built Environment*, *26*(1), 75–88.

Khan, A., & Bradshaw, C. R. (2022). *Quantitative Comparison of the Performance of Vapor Compression Cycles with Various Means of Compressor Flooding*. https://docs.lib.purdue.edu/icec/2739/

Lumpkin, D. R., Bahman, A. M., & Groll, E. A. (2018a). Two-phase injected and vapor-injected compression: Experimental results and mapping correlation for a R-407C scroll compressor. IJR

Marchante-Avellaneda, J., Corberan, J. M., Navarro-Peris, E., & Shrestha, S. S. (2023). A critical analysis of the AHRI polynomials for scroll compressor characterization. *Applied Thermal Engineering*, *219*.

Mathison, M. M., Braun, J. E., & Groll, E. A. (2011). Performance limit for economized cycles with continuous refrigerant injection. *International Journal of Refrigeration*, *34*(1), 234–242.

Moesch, T. W., Bahman, A. M., & Groll, E. A. (2016). *Purdue e-Pubs Performance Testing of a Vapor Injection Scroll Compressor with R407C Performance Testing of a Vapor Injection Scroll Compressor with R407C*.

Navarro, E., Redón, A., Gonzálvez-Macia, J., Martinez-Galvan, I. O., & Corberán, J. M. (2013a). Characterization of a vapor injection scroll compressor as a function of low, intermediate and high pressures and temperature conditions.

Residential Cold Climate Heat Pump Challenge | Department of Energy. (n.d.). Retrieved May 20, 2023, from https://www.energy.gov/eere/buildings/residential-cold-climate-heat-pump-challenge

Tello Oquendo, F. M., Navarro Peris, E., Gonzálvez MacIa, J., & Corberán, J. M. (2016a). Performance of a scroll compressor with vapor-injection and two-stage reciprocating compressor operating under extreme conditions.

Tello-Oquendo, F. M., Navarro-Peris, E., Barceló-Ruescas, F., & Gonzálvez-Maciá, J. (2019). Semi-empirical model of scroll and its extension to describe vapor-injection compressors. Model description and experimental validation.

Tello-Oquendo, F. M., Navarro-Peris, E., & Gonzálvez-Maciá, J. (2017b). Nouvelle méthodologie de caractérisation des compresseurs à spirale à injection de vapeur. *International Journal of Refrigeration*, *74*, 526–537.

Wang, B., Shi, W., Han, L., & Li, X. (2009). Optimization of refrigeration system with gas-injected scroll compressor.

Wang, X., Hwang, Y., & Radermacher, R. (2009a). Two-stage heat pump system with vapor-injected scroll compressor using R410A as a refrigerant. *International Journal of Refrigeration*, *32*(6), 1442–1451.

Winandy, E., Saavedra O, C. S., & Lebrun, J. (2002). Experimental analysis and simplified modelling of a hermetic scroll refrigeration compressor. *Applied Thermal Engineering*, *22*(2), 107–120.

Xu, X., Hwang, Y., & Radermacher, R. (2011). Refrigerant injection for heat pumping/air conditioning systems: Literature review and challenges discussions. *International Journal of Refrigeration*, *34*(2), 402–415.

Yang, M., Wang, B., Li, X., Shi, W., & Zhang, L. (2015). Evaluation of two-phase suction, liquid injection and two-phase injection for decreasing the discharge temperature of the R32 scroll compressor. *IJR*

Yousaf, S., Bradshaw, C., Kamalapurkar, R., San, O., & Bradshaw, C. R. (2022). *Physics Informed Machine Learning Based Reduced Order Model of Unitary Equipment. https://docs.lib.purdue.edu/iracc/2417/*

Ziviani, D., et al. (2018). *Machine Learning Applied to Positive Displacement Compressors and Expanders Performance Mapping*.

ACKNOWLEDGEMENT

The authors would like to acknowledge the Center for Integrated Building Systems, an Industry/University cooperative research center at Oklahoma State University, USA for funding this study.